INNSPUB

International Journal of Agronomy and Agricultural Research (IJAAR)

ISSN: 2223-7054 (Print) 2225-3610 (Online)
http://www.innspub.net
Vol. 21, No. 6, p. 18-27, 2022

RESEARCH PAPER

OPEN ACCESS

Crop yield estimation with irrigation system using remote sensing and machine learning, A case study of Bahawalpur and Rahimyar Khan

Sumaira Hafeez*, Saira Akram, Hassan Hafeez, Waqas Ejaz, Sajid Rashid Ahmad

College of Earth and Environmental Sciences, University of the Punjab, Lahore, Pakistan

Article published on December 06, 2022

Key words: Crop yield, Irrigation system, Remote sensing, Machine learning, Bahawalpur, Rahimyar Khan

Abstract

Different datasets can be used to calculate the cropped areas. These datasets range from Statistical to Physical Measurements and Remotely Sensed. In this study, remotely sensed images were used to identify the cropped areas. RS GIS based Google Earth platform as a mechanical meeting is implemented to sign in unique id regard at each perception area Normalized Difference Vegetation Index (NDVI) the use of Reflectance and intensity of specific limits of data and data collecting instruments Photo-misleadingly Active Radiation (PAR), Fractional Absorbed PAR (fPAR), Absorbed Photo Synthetically in Bahawalpur and Rahim yar khan. The effects are differentiated this observe hopes to convert into the laying out for development of collect assessment from cautious and quantifiable to far flung spotting techniques in Pakistan.

* **Corresponding Author:** Sumaira Hafeez ✉ sumaira.gis@gmail.com

Introduction

Google Earth Engine is a geospatial data handling and administering service. With Earth Engine, one can perform geospatial handling at scale, fueled by Google Cloud Platform. Yield assessment are routinely settled on certified assessments applied at some real data sets made open several time spans after assemble collecting (Zhang, 2016; Shao, 2015; Johnson, 2017). The Normalized Difference Vegetation Index (NDVI) (Mulianga, 2013; Son, 2014; Bulaghi, 2008) is the most frequently utilized distinction file. The collect advancement models use lists determined from somewhat detected information to concentrate on crop improvement at various stages and their yield (DeWit, 2012; Jin, 2017; Xie, 2017). The harvest improvement cycle and yield can be precisely reproduced relying on exact model wellsprings of data, including air conditions, soil conditions and agrarian organization measures (Huang, 2015; Cheng, 2018). As of now, crop advancement models are for the still up in the air by field information and are difficult to add to a local pattern where there is a shortfall of geographical accumulated data (Silvestro *et al.*, 2017; Zhao, 2013).

Materials and methods

Research Significance

- To devise remote sensing methods for estimation of rice cropped area in the districts of Bahawalpur and Rahim Yar Khan.
- To devise methods for estimating rice crop produce in the districts of Bahawalpur and Rahim Yar Khan.
- To automate the procedure of above calculations for further development of the algorithm for scaling at a regional and national level. Google Earth Engine shall be used to implement this task

Study Area

Bahawalpur is organized 889 kilometers for the most part contribute towards the many crops of Pakistan. Outright district of the area is surveyed to connect with 25 thousand square kilometers with a general population thickness of 150 people for each square kilometer. The Rahimyar khan District is fundamental district. It is a piece of the Bahawalpur Division. The District consists water areas to forsake locales. The notable transformation of the five streams, Panjnad, is in like manner a piece of the Rahimyar khan District. Ordinary level more than mean sea level is 586 ft. The hard and fast district of the area is represented to connect with 13 thousand square kilometers with a general population thickness of 420 people for each square kilometer.

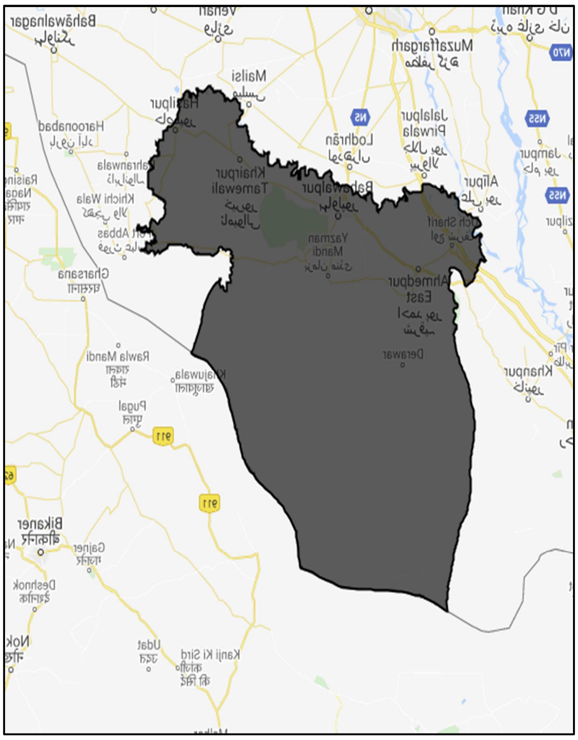

Fig. 1. District map of Bahawalpur.

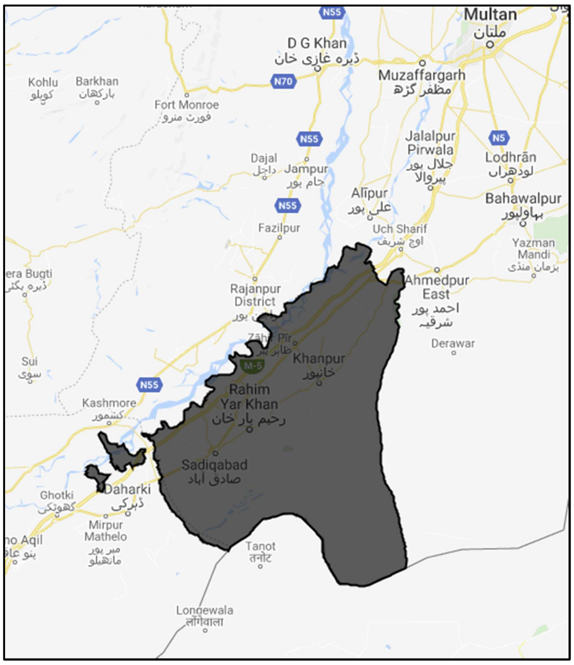

Fig. 2. District map of Rahimyar khan.

Layour

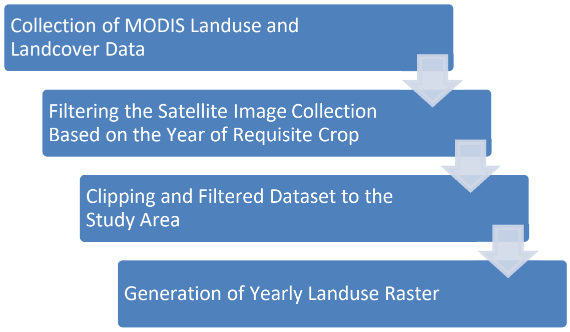

Role of Google Earth Engine and Remote Sensing

By using Google Earth Engine, everyone can do geospatial taking care of at scale, powered by Google Cloud Platform. Google Earth Engine should be visible as a superior execution figuring foundation containing numerous APIs for managing geospatial information or it tends to be seen as an application server for serving clients' numerous intuitive applications. Earth Engine is a phase for representation of logical information. The Earth Engine adds a large number of symbolisms at various handling levels to its datasets consistently which empower the researchers to do upgraded information mining at a worldwide scale. Sentinel-2 was sent off by the European Space Agency. It conveys high goal payload equipped for catching information in various phantom groups. It has a wide area inclusion (290 kilometers).

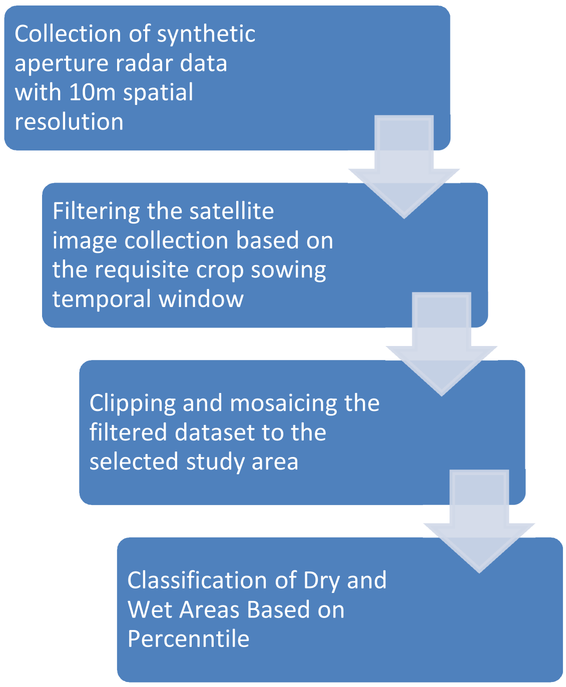

Data Acquisition

Every element is the polygonal quarter encased through inner cutoff factors and out of doors beaches in which applicable, and numerous international locations incorporate numerous features, one for every disjoint region. All of the 180,741 blueprints are part of the region of one of the 284 international locations depicted on this dataset

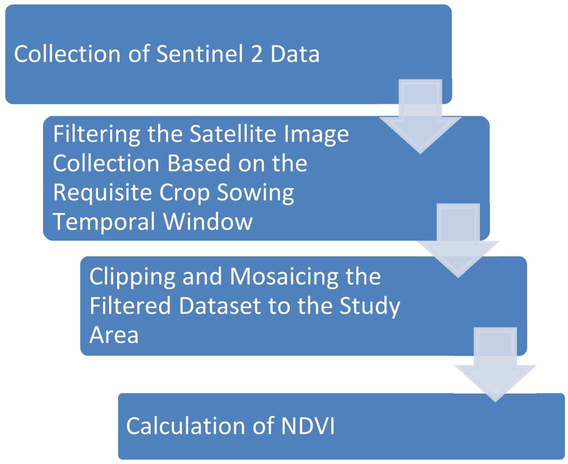

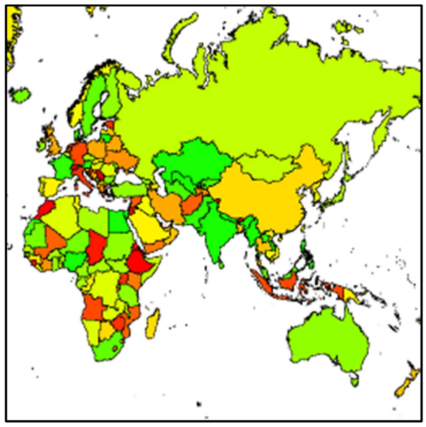

Fig. 3. LSIB country boundaries.

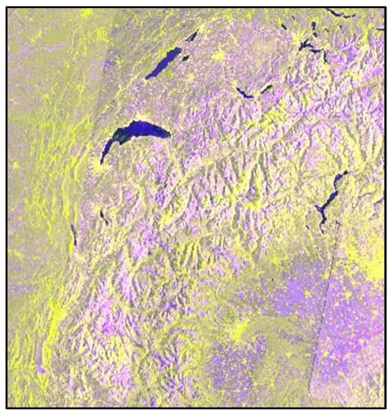

Fig. 4. SAR data.

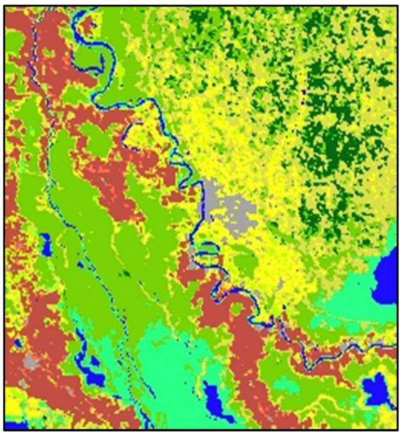

Fig. 5. MODIS global land cover.

Results and discussions

Land Cover Classification

land cover grouping is a fundamental piece of distinguishing proof of yields through remote detecting. Because of un-accessibility of a public data set. The information used in the ongoing review was gathered from various resources

Wet and Dry Areas Estimation

The wet regions were distinguished utilizing the most minimal tenth percentile of the backscatter saw by the satellite. The dry regions were distinguished utilizing the most noteworthy tenth percentile of the backscatter saw by the satellite. It was seen that because of the calculation being applied to individual pictures, rather than the mosaic in general.

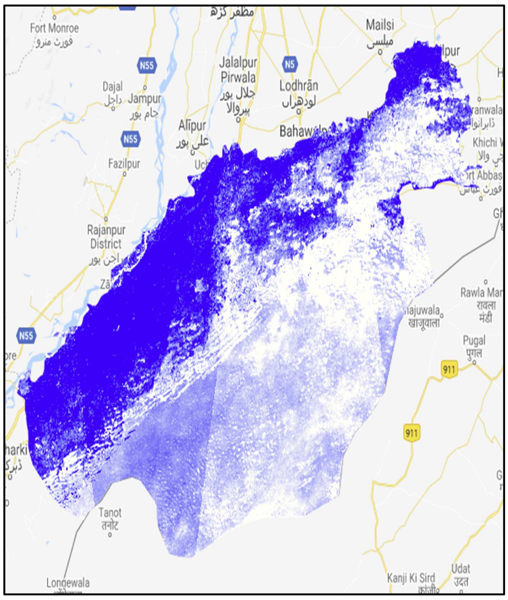

Fig. 6. 10th percentile wet area.

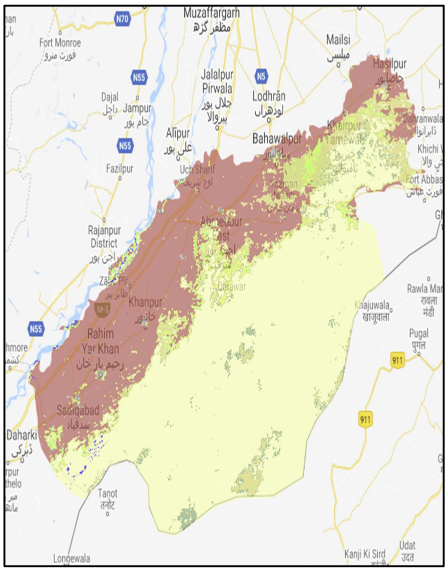

Fig. 7. Land use classification.

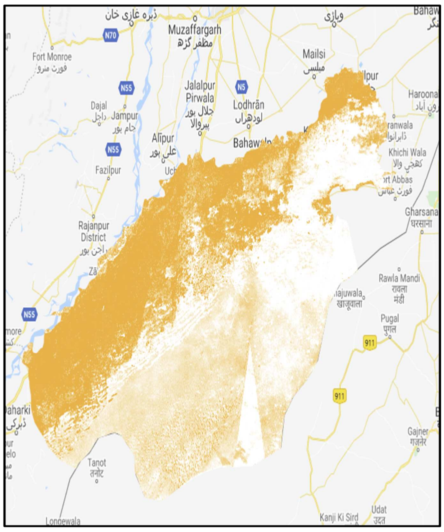

Fig. 8. 10th percentile dry areas.

Identification of Wet Rice Zones

The rice regions characterized by most noteworthy likelihood were recognized by taking away the presumably wet regions from the most likely dry regions utilizing straightforward picture deduction. Individual picture mosaic lines were again seen because of the way that pictures are mosaic-ed after the estimation work has been applied.

NDVI Calculation

To produce the NDVI of the review region in the harvest planting fleeting window, comparative strategy for handling the Sentinel 2 information is utilized. Be that as it may, for this situation Near Infrared (NIR) and Red (R) groups are utilized for computing the standardized distinction vegetation list.

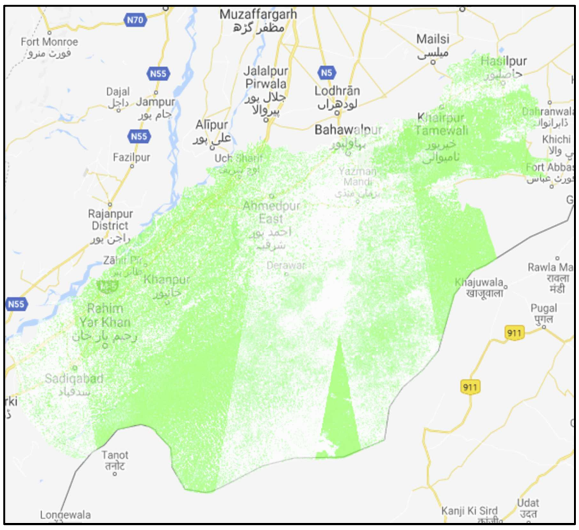

Fig. 9. Probable wet rice field areas.

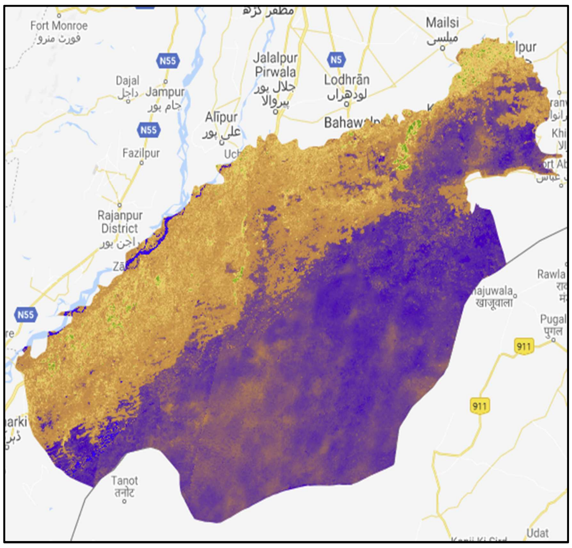

Fig. 10. NDVI calculated in sowing period.

Wet Zones for Cropped Zones

The likely wet rice, right off the bat, fields were joined. The outcomes got from the explained for an enormous scope in maps (Kuri, 2014; Ban, 2017; Holzman, 2014).

Land Use, Wet Areas and NDVI for Cropped Areas

As revealed by different researchers, a NDVI of under 1 at the time planting can be utilized. A similar model was used to sift through all the area having NDVI is more noteworthy than one at the time-frame of the yield being contemplated.

f_PAR Processing and Mapping

Albeit the Google Earth Engine allows us to finish the coping with without imagining the statistics, the imported statistics from numerous satellites is first imported and its genuineness is checked by envisioning something very similar. Since the f_PAR dataset is imported as an assortment, a middle of the gathered information is pictured by adding the assortment into the guide (Bandaru, 2013; Lobell, 2003; Xin, 2013).

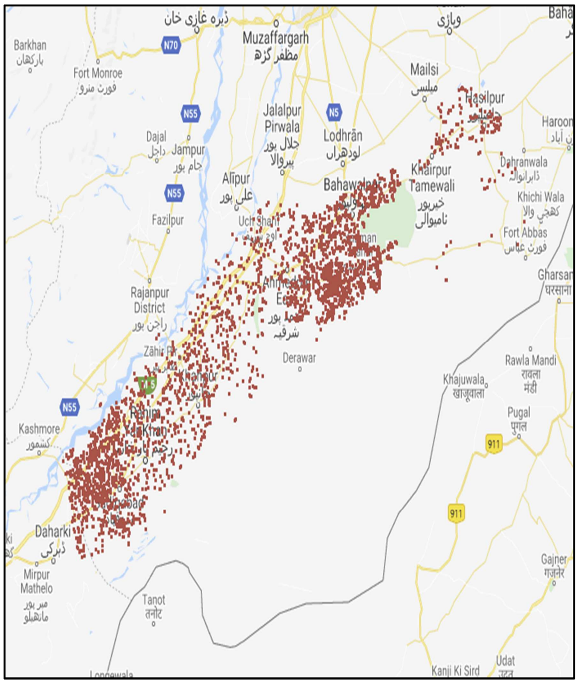

Fig. 11. Probable wet rice.

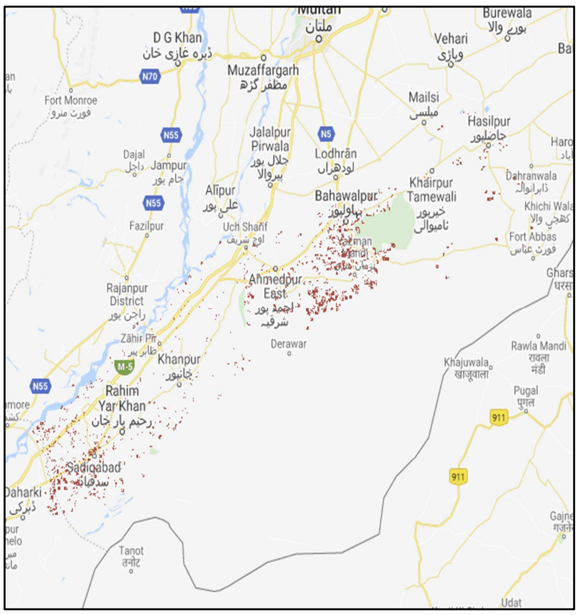

Fig. 12. NDVI filtration.

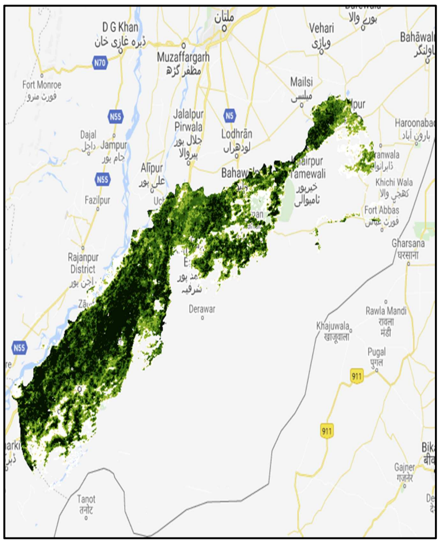

Fig. 13. Median f_{PAR}.

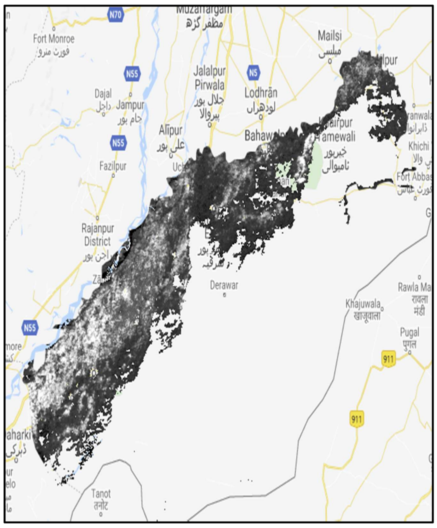

Fig. 15. Monthly APAR.

Photo synthetically Active Radiation (PAR)

The net shortwave radiation transition is separated from the information and scaled regarding the hypothesis. The said information is acquired with a fleeting goal of multi month, and is cut to the limit of the review region (Bandaru, 2013; Lobell, 2003; Xin, 2013).

Wind Power

Crop Biomass is then determined utilizing the google earth engine pictures registered over the yield time duration. Pictures from fleeting assortment of google earth engine are then aggregated into a solitary picture assortment, arranged with the duration of the assortment alongside the light use proficiency. A visual portrayal where blue regions address the fields with the most elevated biomass gathered though red regions address least biomass amassing.

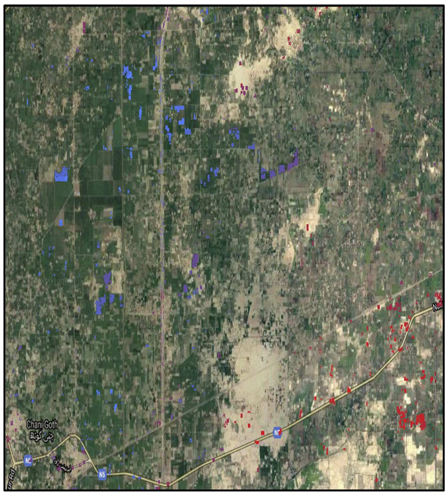

Fig. 16. Accumulated biomass.

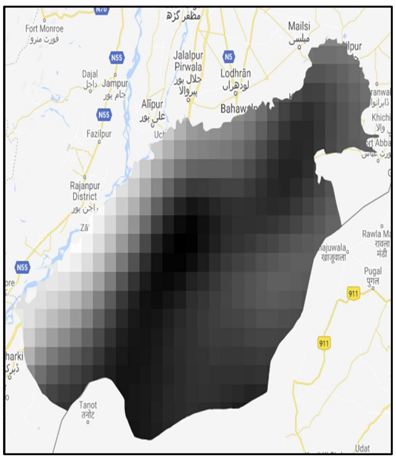

Fig. 14. Median net shortwave flux.

The results obtained using the novel approach differ by the estimated amounts of crop reporting service, Punjab by -3% in identification of rice cropped area and 28.8% for the crop produce achieved from said areas.

Table 1. Summary of Results for the Year 2018-2019.

Description	Crop Reporting Service, Punjab in the year 2018	Statistics gathered from current study in the year 2018	Percentage Difference in 2018
Area cropped for Rice in Study Districts	307.6 sq. km	298 sq. km	-3%
Estimated Produce	65.39 Thousand Tonnes	84.24 Thousand Tonnes	28.8%

Same algorithm was applied for the year 2019-20. A difference of -36% in identification of crops and -17% in produce was observed.

Table 1. Summary of Results for the Year 2019-2020.

Description	Crop Reporting Service, Punjab in the year 2019	Statistics gathered from current study in the year 2019	Percentage Difference in 2019
Area cropped for Rice in Study Districts	339 sq. km	214 sq. km	-36%
Estimated Produce	73.56 Thousand Tonnes	60.84 Thousand Tonnes	-17%

Since the algorithm developed can be applied to any year by only changing the year of study in the code, results for the year 2017-2018 were also obtained and are summarized in table

Table 2. Summary of Results for the Year 2017-2018.

Description	Crop Reporting Service, Punjab in the year 2018	Statistics gathered from current study in the year 2018	Percentage Difference in 2018
Area cropped for Rice in Study Districts	307.4 sq. km	182 sq. km	-40%
Estimated Produce	58 Thousand Tonnes	58.46 Thousand Tonnes	0.8%

Conclusions

The fPAR statistics assembled from remotely sensed data sets. While overseeing crop fields at a greater confined size, this dataset brought on issues; However, it's far predicted that for a survey location having diverse yields with a more property district, the computation will paintings perfectly, but that isn't always what goes on whilst overseeing farms on a community or public scale. The evaluation of transferring closer to solar organized from the remotely sensed imagery is furthermore at a low spatial goal of round 1km; which once more impacts effects from fields in which property sizes are in or 3 segments of land, maximum perfect situation.

References

Awad. 2019. Toward Precision in Crop Yield Estimation Using Remote Sensing and Optimization Techniques. Agriculture **9(3),** 54-57.

Balaghi R, Tychon B, Eerens H, Jlibene. 2008. Empirical regression models using NDVI, rainfall and temperature data for the early prediction of wheat grain yields in Morocco. Int. J. Appl. Earth Obs. Geoinf **10,** 438-452.

Ban H, Kim K, Park N, Lee. 2017. Using MODIS Data to Predict Regional Corn Yields. Remote Sens **9,** 16-26.

Bandaru V, West TO, Ricciuto DM, César. 2013. Estimating crop net primary production using national inventory data and MODIS-derived parameters. ISPRS J. Photogram. Remote Sens **80,** 61-71.

Bioresita F, Puissant A, Stumpf A, Malet. 2018. A Method for Automatic and Rapid Mapping of Water Surfaces from Sentinel-1 Imagery. Remote Sensing **10(2),** 217-227.

Bolton DK, Friedl. 2013. Forecasting crop yield using remotely sensed vegetation indices and crop phenology metrics. Agric. For. Meteorol **173,** 74-84.

Cheng Z, Meng J, Qiao Y, Wang Y, Dong W, Han. 2018. Preliminary study of soil available nutrient simulation using a modified WOFOST model and time-series remote sensing observations. Remote Sens **10,** 64-71.

Clauss K, Ottinger M, Kuenzer. 2017. Mapping rice areas with Sentinel-1 time series and super pixel segmentation. International Journal of Remote Sensing **39(5),** 1399-1420.

Cunha M, Marçal ARS, Silva. 2010. Very early prediction of wine yield based on satellite data from Vegetation. Int. J. Remote Sens **31,** 3125-3142.

DeWit A, Duveiller G, Defourny. 2012. Estimating regional winter wheat yield with WOFOST through the assimilation of green area index retrieved from MODIS observations. Agric. For. Meteorol **164,** 39-52.

Doktor D, Bondeau A, Koslowski D, Badeck. 2009. Influence of heterogeneous landscapes on computed green-up dates based on daily AVHRR NDVI observations. Remote Sens Environ **113,** 2618-2632.

Fernandez-Ordoñez YM, Soria-Ruiz. 2017. Maize crop yield estimation with remote sensing and empirical models. In Proceedings of the IEEE International Geoscience and Remote Sensing Symposium, Fort Worth, TX, USA, 23-28 July 2017, IEEE: Piscataway, NJ, USA, 2017.

Fieuzal R, Marais SC, Baup. 2017. Estimation of corn yield using multi-temporal optical and radar satellite data and artificial neural networks. Int. J. Appl. Earth Obs. Geoinf **57,** 14-23.

Frouin R, Pinker. 1995. Estimating Photosynthetically active radiation (PAR) at the Earth's Surface from satellite Observations. Journal of Remote Sensing of Environment **51,** 98-107.

Holzman ME, Rivas R, Piccolo. 2014. Estimating soil moisture and the relationship with crop yield using surface temperature and vegetation index. Int. J. Appl. Earth Obs. Geoinf **28,** 181-192.

Huang J, Ma H, Su W, Zhang X, Huang Y, Fan J, Wu. 2015. Jointly assimilating MODIS LAI and ET products into the SWAP model for winter wheat yield estimation. IEEE J. Sel. Top. Appl. Earth Obs. Remote Sens **8,** 4060-4071.

Hutchinson. 1991. Uses of satellite data for famine early warning in sub-Saharan Africa. Int. J. Remote Sens **12,** 1405-1421.

Jin X, Li Z, Yang G, Yang H, Feng H, Xu X, Wang J, Li X, Luo. 2017. Winter wheat yield estimation based on multi-source medium resolution optical and radar imaging data and the Aqua Crop model using the particle swarm optimization algorithm. ISPRS J. Photogram Remote Sens **126,** 24-37.

Johnson. 2014. An assessment of pre- and within-season remotely sensed variables for forecasting corn and soybean yields in the United States. Remote Sens. Environ **141,** 116-128.

Johnson MD, Hsieh WW, Cannon AJ, Davidson A, Bédard. 2016. Crop yield forecasting on the Canadian Prairies by remotely sensed vegetation indices and machine learning methods. Agric. For. Meteorol **218-219,** 74-84.

Karnieli 2003. Natural vegetation phenology assessment by ground spectral measurements in two semi-arid environments. Int. J. Biometeorol **47,** 179-187.

Kasampalis D, Alexandridis T, Deva C, Challinor A, Moshou D, Zalidis. 2018. Contribution of Remote Sensing on Crop Models: A Review. Journal of Imaging **4(4),** 52-61.

Kowalik W, Dabrowska ZK, Meroni M, Raczka TU, de Wit. 2014. Yield estimation using SPOT-VEGETATION products: A case study of wheat in European countries. Int. J. Appl. Earth Obs. Geoinf **32,** 228-239.

Kuri F, Murwira A, Murwira KS, Masocha. 2014. Predicting maize yield in Zimbabwe using dry dekads derived from remotely sensed Vegetation Condition Index. Int. J. Appl. Earth Obs. Geoinf **33,** 39-46.

Lobell DB, Asner GP, Ortiz-Monasterio JI, Benning. 2003. Remote sensing of regional crop production in the Yaqui Valley, Mexico: Estimates and uncertainties. Agric. Ecosystem. Environ **94,** 205-220.

Ma G, Huang J, Wu W, Fan J, Zou J, Wu. 2013. Assimilation of MODIS-LAI into the WOFOST model for forecasting regional winter wheat yield. Math. Compute. Model **58,** 634-643.

Ma YP, Wang SL, Zhang L, Hou YY, Zhuang LW, He YB, Wang. 2008. Monitoring winter wheat growth in North China by combining a crop model and remote sensing data. Int. J. Appl. Earth Obs. Geoinf **10,** 426-437.

Methodology of Crop Estimate, Pakistan Bureau of Statistics, Available Online: http://www.pbs.gov.pk /content/methodology-crop-estimate

Methods for measuring crop area and yield, Food and Agriculture Organization. 2018. Available Online: http://gsars.org/wp-content/ uploads/ 2018/10/GS-CROPS-BROCHURE-EN-04.pdf

Mulianga B, Bégué A, Simoes M, Todoroff. 2013. Forecasting regional sugarcane yield based on time integral and spatial aggregation of MODIS NDVI. Remote Sens **5,** 2184-2199.

Norman JM, Kustas WP, Humes. 1995. Source approach for estimating soil and vegetation energy fluxes from observation of directional radiometric surface temperature. Agric. Forest. Meteorol **77,** 263-293.

Noureldin NA, Aboelghar MA, Saudy HS, Ali. (2013). Rice yield forecasting models using satellite imagery in Egypt. Egypt. J. Remote Sens. Space Sci. **16,** 125-131.

Peng D, Huang J, Li C, Liu L, Huang W, Wang F, Yang. 2014. Modelling paddy rice yield using MODIS data. Agric. For. Meteorol **184,** 107-116.

Piao SL, Fang JY, Zhou LM, Ciais P, Zhu B. 2006. Variations in satellite-derived phenology in China's temperate vegetation. Glob Change Biol **12,** 672-685.

Ruimy A, Kergoat L, Bondeau Inter-comparison ThEPOF ThE. 1999. Comparing global models of terrestrial net primary productivity (NPP): analysis of differences in light absorption and light-use efficiency. Global Change Biology **5(S1),** 56-64.

Shao Y, Campbell JB, Taff GN, Zheng. 2015. An analysis of cropland mask choice and ancillary data for annual corn yield forecasting using MODIS data. Int. J. Appl. Earth Obs. Geoinf **38,** 78-87.

Silvestro P, Pignatti S, Pascucci S, Yang H, Li Z, Yang G, Huang W, Casa. 2017. Estimating Wheat Yield in China at the Field and District Scale from the Assimilation of Satellite Data into the Aquacrop and Simple Algorithm for Yield (SAFY) Models. Remote Sens **9,** 509-516.

Skakun S, Franch B, Vermote E, Roger J, Becker RI, Justice C, Kussul. 2017. Early season large-area winter crop mapping using MODIS NDVI data, growing degree days' information and a Gaussian mixture model. Remote Sens. Environ **195,** 244-258.

Son NT, Chen CF, Chen CR, Minh VQ, Trung. 2014. A comparative analysis of multitemporal MODIS EVI and NDVI data for large-scale rice yield estimation. Agric. For. Meteorol **197,** 52-64.

Stöckli R, Vidale. 2004. European plant phenology and climate as seen in a 20-year AVHRR land-surface parameter dataset. Int J Remote Sens **25,** 3303-3330.

Tucker CJ, Slayback DA, Pinzon JE, Los SO, Myneni RB, Taylor MG. 2001. Higher northern latitude normalized difference vegetation index and growing season trends from 1982 to 1999. Int J Biometeorol **45,** 184-190.

Valero S, Ceccato P, Baethgen WE, Chanussot. 2013. Identification of agricultural crops in early stages using remote sensing images. 2013 IEEE International Geoscience and Remote Sensing Symposium - IGARSS. IGARSS 2013 - 2013 IEEE International Geoscience and Remote Sensing Symposium.

Wang L, Zhang F, Jing Y, Jiang X, Yang S, Han. 2014. Multi-Temporal Detection of Rice Phenological Stages Using Canopy Spectrum. Rice Science **21(2),** 108-115.

White MA, de Beurs KM, Didan K, Inouye DW, Richardson AD, Jensen OP, Okeefe J, Zhang G, Nemani R, van Leeuwen WJD, Brown JF, de Wit A, Schaepman M, Lin X, Dettinger M, Bailey AS, Kimball J, Schwartz MD, Baldocchi D, Lee JT, Lauenroth WK. 2009. Inter-comparison, interpretation, and assessment of spring phenology in North America estimated from remote sensing for 1982-2006. Glob Change Biol **15,** 2335-2359.

World Food Program. 2020. The State of Food Security and Nutrition in the World (SOFI) Report. Available online: https://www.wfp.org/content/2017-state-food-security-and-nutrition-world-sofi-report (accessed on 20 August).

Xie Y, Wang P, Bai X, Khan J, Zhang S, Li L, Wang. 2017. Assimilation of the leaf area index and vegetation temperature condition index for winter wheat yield estimation using Landsat imagery and the CERES-Wheat model. Agric. For. Meteorol **246,** 194-206.

Xin Q, Gong P, Yu C, Yu L, Broich M, Suyker A, Myneni. 2013. A production efficiency model-based method for satellite estimates of corn and soybean yields in the Midwestern US. Remote Sens **5,** 5926-5943

Yu B, Shang. 2018. Multi-Year Mapping of Major Crop Yields in an Irrigation District from High Spatial and Temporal Resolution Vegetation Index. Sensors **18(11),** 37-87.

Zhang X, Zhang. 2016. Monitoring interannual variation in global crop yield using long-term AVHRR and MODIS observations. ISPRS J. Photogram. Remote Sens **114,** 191-205.

Zhao Y, Chen S, Shen. 2013. Assimilating remote sensing information with crop model using Ensemble Kalman Filter for improving LAI monitoring and yield estimation. Ecol. Model **270,** 30-42.

Zhong L, Hu L, Yu L, Gong P, Biging GS. 2016. Automated mapping of soybean and corn using phenology. ISPRS J. Photogram. Remote Sens **119,** 151-164.